Roger N. Rosenberg
Editor

Atlas of Clinical Neurology

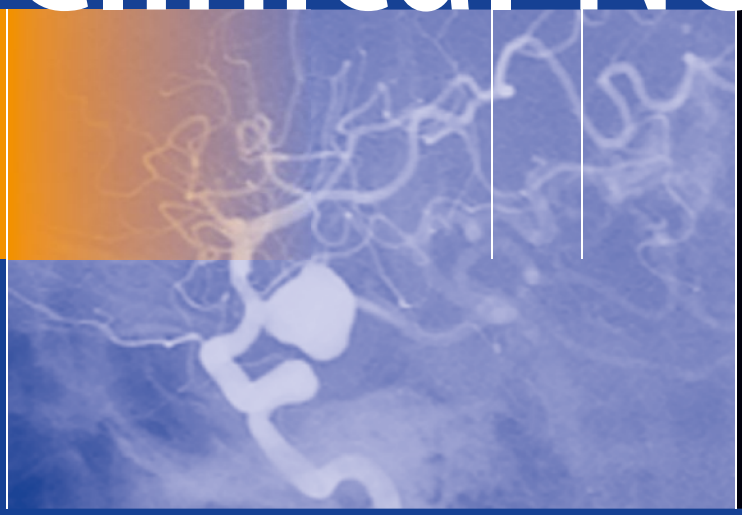

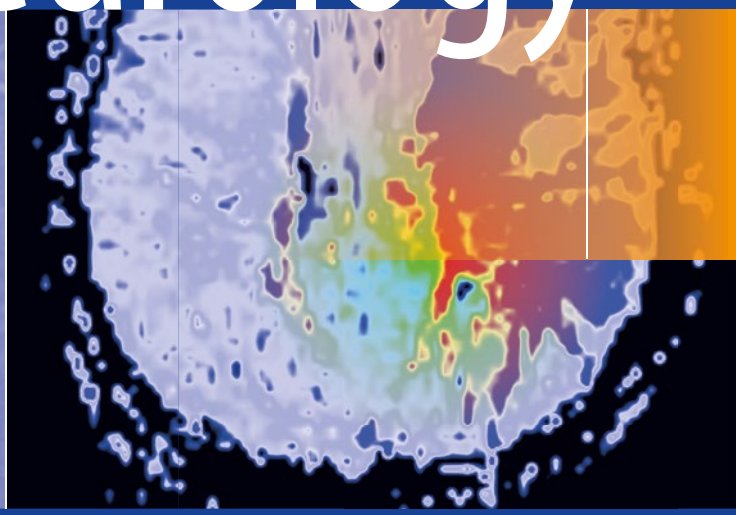

Fourth Edition

Springer

Atlas of Clinical Neurology

Roger N. Rosenberg
Editor

Atlas of Clinical Neurology

Fourth Edition

Springer

Editor
Roger N. Rosenberg
University of Texas Southwestern Medical Center
Dallas, TX
USA

ISBN 978-3-030-03281-4 ISBN 978-3-030-03283-8 (eBook)
https://doi.org/10.1007/978-3-030-03283-8

This Springer imprint is published by the registered company Springer Nature Switzerland AG
The registered company address is: Gewerbestrasse 11, 6330 Cham, Switzerland

Preface

The Fourth Edition of the *Atlas of Clinical Neurology* highlights and underscores the enormous strides being made in the biologic understanding of neurologic disease. Neurology is a highly visual specialty. The neurologic examination, magnetic resonance imaging (MRI), electroencephalography (EEG), positron emission tomographic (PET) scanning, functional MRI (fMRI), and light microscopy and electron microscopy are examples of visual images that define neurologic disease and normal brain functions.

This *Atlas of Clinical Neurology* has been designed to provide a comprehensive pictorial and visual exposition and integration of all aspects of neurologic disease, including clinical syndromes, and related neuropathology, neuroradiology, neurophysiology, neuropharmacology, neurochemistry, and molecular biology. The goal is to provide a holistic visual concept of neurologic disease to allow the clinician an overall image of a specific neurologic disorder.

Quality patient management requires the good judgment and factual knowledge of an experienced physician. The *Atlas of Clinical Neurology* is intended to provide essential information about neurologic disease in an immediate and integrated manner to help the neurologist in the primary function of providing excellence in patient care.

There has been great progress in the past decade in our understanding of the cellular, genetic, genomic, and molecular basis of many neurologic diseases. As a result, each chapter has been revised and updated to reflect these advances, including new therapies that have been developed as a result of this recent knowledge. Thrombolytic and endovascular therapy for stroke, deep brain stimulation for Parkinson's disease, new classes of anticonvulsants, and effective immune therapy for multiple sclerosis and paraneoplastic and autoimmune disorders represent examples of recent significant therapeutic advances in neurology.

Of great importance to the understanding of gene structure and function in the nervous system have been discoveries in DNA triplet repeat expansions, including Huntington's disease, and the autosomal dominant spinocerebellar degenerations: Machado-Joseph disease (*SCA3*), the most common autosomal dominant ataxia worldwide, dentatorubropallidoluysian atrophy, fragile X disease, myotonic muscular dystrophy, and Friedreich's ataxia**.**

The leading cause of dementia in our society – affecting over 5 million Americans and countless millions more around the world – Alzheimer's disease (AD), has been shown to be a clinical syndrome due to specific different genetic mutations in selected families with dominantly inherited disease. Rare mutations in the amyloid precursor protein gene (chromosome 21), the presenilin 1 gene (chromosome 14), and the presenilin 2 gene (chromosome 1) result in dominantly inherited AD. A major risk factor for AD is the presence of the E4 allele of apolipoprotein E (chromosome 19). Recently, 100 highly polymorphic genes were identified that increase the risk for late-onset AD. Many unique polymorphic genotypes result in a wide spectrum of phenotypic AD.

Additional detailed images related to the dementias are included in this Fourth Edition. These clinical-molecular correlations are all very recent and attest to the scientific vigor of current neuroscientific research. It is my view that these new data will lead in the near future to effective new therapy for AD that will slow its rate of progress and significantly reduce the incidence of this major debilitating disease.

Brain scanning with PET and fMRI has effectively defined regional brain areas for behaviors. The clarity of insights into heterogeneous brain functions by PET and MRI is literally revolutionizing our concepts about human cognition.

The topics covered in this *Atlas* represent the most common and important neurologic diseases, and each chapter is authored by authorities in the field. The descriptive text for each disease sets the stage for the use of the detailed images both for self-instruction and for lecture presentations. Several hundred images, algorithms, tables, and schematic drawings have been selected carefully for their clarity in conveying the essence of a particular disorder. The collection of figures for a specific disease is intended to provide a thorough and comprehensive description that enables the clinician to generate a clear concept of current thinking about the pathogenesis of that disorder and finally a framework for rational therapy.

I am grateful to my colleagues for conceptualizing the *Atlas* with me initially and for updating the Fourth Edition. Our overall educational objective of integrating illustrated text with well-focused images to provide the final detailed visual imprint of each neurologic disorder has been achieved. We believe our efforts provide highly useful educational material for the student and teacher alike.

I wish to recognize and express our appreciation and gratitude to Lee Klein, developmental editor at Springer, for his considerable skills and insights in developing this update of the *Atlas*.

It is our hope that the *Atlas of Clinical Neurology* will be of value to neurologists and physicians of all specialties caring for patients with neurologic disorders, as well as to neurologic investigators and teachers of neurology, and in the final analysis, we hope that it will benefit our patients.

Dallas, TX, USA

Roger N. Rosenberg, MD

Contents

List of Contributors

Lucia L. Balos, MD Department of Pathology and Anatomical Sciences, Jacobs School of Medicine & Biomedical Sciences, Buffalo General Hospital, Buffalo, NY, USA

Rachel B. Beekman, MD Department of Neurology, Yale School of Medicine, New Haven, CT, USA

Alma R. Bicknese, MD Ann & Robert H. Lurie Children's Hospital of Chicago, Chicago, IL, USA

Thomas D. Bird, MD Department of Neurology, University of Washington, Seattle, WA, USA

Geriatric Research Education and Clinical Center, VA Puget Sound Health Care System, Seattle, WA, USA

Carsten G. Bönnemann, MD Porter Neuroscience Research Center, Bethesda, MD, USA

Kimiko Domoto-Reilly, MD Department of Neurology, University of Washington, Seattle, WA, USA

Marthand Eswara, MD Sutter Children's Services, Sacramento, CA, USA

Stanley Fahn, MD Department of Neurology, Columbia University Medical Center, New York, NY, USA

Glen A. Fenton, MD Department of Neurology, Saint Louis University, St. Louis, MO, USA

Edward J. Fine, MD Department of Neurology, Jacobs Neurological Institute, Williamsville, NY, USA

Karen L. Fink, MD, PhD Baylor Scott and White Neuro-Oncology Associates, Dallas, TX, USA

Margaret E. Flanagan, MD Department of Laboratory Medicine and Pathology, University of Minnesota, Minneapolis, MN, USA

Blair Ford, MD Department of Neurology, Columbia University, Neurological Institute, New York, NY, USA

Thomas J. Geller, MD SSM Cardinal Glennon Children's Hospital, St. Louis, MO, USA

Thomas J. Grabowski Jr. Neurology Clinic, University of Washington Medical Center, Seattle, WA, USA

Dorothy K. Grange, MD Department of Pediatrics, Washington University in St. Louis School of Medicine, St. Louis, MO, USA

Paul E. Greene, MD Department of Neurology, Mt. Sinai Medical Center, New York, NY, USA

David M. Greer, MD, MA Department of Neurology, Boston University School of Medicine, Boston, MA, USA

Shamir Haji, MD Neuroscience Intensive Care Unit, Fort Sanders Regional Medical Center, Knoxville, TN, USA

Yousef Hannawi, MD Neurological Institute, Wexner Medical Center, The Ohio State University, Columbus, OH, USA

Anita J. Huttner, MD Department of Pathology, Brady Memorial Laboratory, Yale School of Medicine, New Haven, CT, USA

Suman Jayadev, MD Department of Neurology, University of Washington, Seattle, WA, USA

Michele H. Johnson, MD Department of Radiology and Biomedical Imaging, Yale School of Medicine, New Haven, CT, USA

Burk Jubelt, MD Departments of Neurology, Microbiology/Immunology, and Neuroscience, SUNY Upstate Medical University, Syracuse, NY, USA

Suresh Kotagal, MD Departments of Neurology and Pediatrics, Mayo Clinic, Rochester, MN, USA

Marc E. Lenaerts, MD Department of Neurology, UC Davis Medical Center, Sacramento, CA, USA

Marek A. Mirski, MD, PhD Department of Anesthesiology & Critical Care Medicine, Johns Hopkins Medicine, Baltimore, MD, USA

Michael A. Nigro, DO Farmington Hills**,** MI**,** USA

Joseph E. Parisi, MD Department of Laboratory Medicine and Pathology, Mayo Clinic, Rochester, MN, USA

Thomas Pittman, MD Department of Neurosurgery and Pediatrics, University of Kentucky Hospital, Lexington, KY, USA

Elisabeth J. Rushing, MD Institute for Neuropathology, University Hospital Zurich, Zurich, Switzerland

Jharna N. Shah, MD Neurological Critical Care, Tower Health Medical Group, West Reading, PA, USA

Hyung Sub Shim, MD Department of Neurology, University of Iowa Hospitals and Clinics, Iowa City, IA, USA

Nicholas J. Silvestri, MD Department of Neurology, Jacobs School of Medicine and Biomedical Sciences, Buffalo, NY, USA

Laura E. Simionescu, MD Department of Neurology, SUNY Upstate Medical University, Syracuse, NY, USA

Michael R. Swenson, MD, MSc Lander Medical Clinic, Lander, WY, USA

Daniel Tranel, PhD Department of Neurology, University of Iowa Hospitals and Clinics, Iowa City, IA, USA

Paul C. Van Ness, MD Department of Neurology, Baylor College of Medicine, Houston, TX, USA

Gil I. Wolfe, MD Department of Neurology, Jacobs School of Medicine and Biomedical Sciences, SUNY University, Buffalo, Buffalo, NY, USA

Lily Wong-Kisiel, MD Division of Child Neurology, Division of Epilepsy, Department of Neurology, Mayo Clinic, Rochester, MN, USA

Earl A. Zimmerman, MD Department of Neurology, Albany Medical College, Albany, NY, USA

Developmental Disorders

Suresh Kotagal, Alma R. Bicknese, Marthand Eswara, Glen A. Fenton, Thomas J. Geller, Dorothy K. Grange, Michael A. Nigro, Joseph E. Parisi, Thomas Pittman, and Lily Wong-Kisiel

This chapter covers a varied group of disorders that develop as a consequence of genetic abnormalities, prenatal or perinatal infections, ischemia, or uncertain etiology. All lead to abnormal development of the nervous system. Some disorders have been selected because of the challenge they pose in diagnosis and management, and others because they illustrate important concepts in neurodevelopment or pathophysiology.

Advances in molecular genetics and neuroimaging play an ever-increasing role in furthering our understanding of congenital central nervous system malformations. A thorough general physical examination provides valuable diagnostic information in infants and children who present with seizures and developmental delay. Nowhere is this principle more important than in connection with the *phakomatoses*, clues to the specific diagnosis of which may become apparent during a careful general physical examination. We now also have a better understanding of the mechanisms underlying abnormal cell proliferation, angiogenesis, and synaptogenesis, and synaptic organization in neurocutaneous syndromes such as tuberous sclerosis and neurofibromatosis. As a general rule, the more severe the disturbance of brain development, the earlier is the onset of clinical symptoms. Thus, seizures, microcephaly, macrocephaly, hemiparesis, external defects, and developmental delay regularly accompany developmental disorders presenting in infancy or early childhood.

Myelomeningocele

About 1 child in 1000 is born with a myelomeningocele (Fig. 1). Symptoms vary depending on the level of the lesion. Bowel and bladder dysfunction is nearly universal, but motor disability varies with the level of the spinal cord lesion; that is, children with thoracic lesions have flaccid paraplegia, whereas those with lumbar lesions have various degrees of lower extremity weakness. Almost all affected children have hydrocephalus, given the association with Chiari type II malformation; some may show macrocephaly apparent at birth, but others do not develop signs of intracranial hypertension until the myelomeningocele has been surgically closed.

S. Kotagal (✉)
Departments of Neurology and Pediatrics, Mayo Clinic, Rochester, MN, USA
e-mail: kotagal.suresh@mayo.edu

A. R. Bicknese
Ann & Robert H. Lurie Children's Hospital of Chicago, Chicago, IL, USA
e-mail: alma.bicknese@northwestern.edu

M. Eswara
Sutter Children's Services, Sacramento, CA, USA
e-mail: meswara@sutterhealth.org

G. A. Fenton
Department of Neurology, Saint Louis University, St. Louis, MO, USA
e-mail: glen.fenton@slu.edu

T. J. Geller
SSM Cardinal Glennon Children's Hospital, St. Louis, MO, USA
e-mail: gellertj@slu.edu

D. K. Grange
Department of Pediatrics, Washington University in St. Louis School of Medicine, St. Louis, MO, USA
e-mail: grangedk@wustl.edu

M. A. Nigro
Farmington Hills, MI, USA

J. E. Parisi
Department of Laboratory Medicine and Pathology, Mayo Clinic, Rochester, MN, USA
e-mail: parisi.joseph@mayo.edu

T. Pittman
Department of Neurosurgery and Pediatrics, University of Kentucky Hospital, Lexington, KY, USA
e-mail: Tpitt2@uky.edu

L. Wong-Kisiel
Division of Child Neurology, Division of Epilepsy, Department of Neurology, Mayo Clinic, Rochester, MN, USA
e-mail: wongkisiel.lily@mayo.edu

R. N. Rosenberg (ed.), *Atlas of Clinical Neurology*, https://doi.org/10.1007/978-3-030-03283-8_1

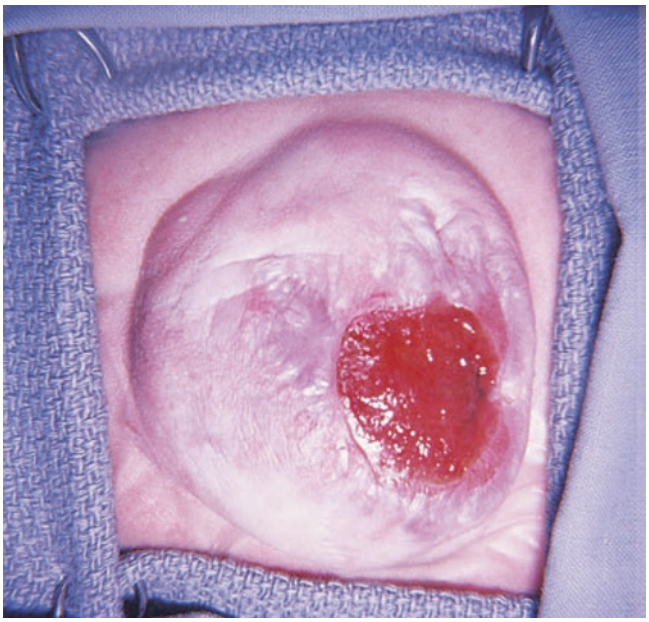

Fig. 1 A myelomeningocele

The treatment of children with myelomeningoceles that require intervention involves back closure, usually performed within the first 24 h of life; delay beyond that time increases the likelihood of infection. A ventriculoperitoneal shunt can be placed at the same time, but many neurosurgeons prefer to perform the two procedures separately intrauterine repair. Many children will have problems with bony deformity and contractures, and almost all with higher lesions ultimately develop scoliosis. Recurrent urinary tract infections, vesicoureteral reflux associated with a spastic bladder, and problems with continence and sexual function are also common. Sleep-disordered breathing, consisting of a combination of hypoventilation and central and obstructive sleep apnea, may lead to daytime fatigue and pulmonary hypertension. Finally, as they grow, some patients with myelomeningocele become symptomatic from tethering of the spinal cord that is manifested by back pain, progressive weakness, and changes in bowel and bladder habits. Symptomatic tethering usually requires operative intervention.

Research on the effect of periconceptual folic acid supplementation of the mother offers some hope for prevention, but presently the disorder continues to occur in the United States at an incidence of 0.5–1 per 1000 pregnancies.

Anencephaly

Anencephaly (Fig. 2) and other neural tube defects can be diagnosed prenatally through maternal serum alpha-fetoprotein screening (elevated) and fetal ultrasonography. The defect results from failed closure of the anterior neuropore in the neural tube. All cases of anencephaly should be detectable by ultrasonography by 14 weeks of gestation with state-of-the-art equipment. After the first affected offspring, the recurrence risk for any neural tube defect in a subsequent pregnancy is approximately 4%. Neural tube defects are multifactorial in etiology, with a group of genes inherited from each parent acting in association with environmental factors to cause the defect. Maternal folic acid deficiency can contribute to the incidence of neural tube defects. For women who have had a previous child with a neural tube defect, the consumption of folic acid, 4000 μg (4 mg) per day, can reduce the recurrence risk to 0.5–1%. To reduce the overall incidence of neural tube defects, it is now recommended that all women of childbearing age ingest folic acid, 0.4 mg to 0.8 mg/day. Since the average intake of dietary folic acid is about 0.2 mg/d, government agencies are recommending periconceptional maternal folic acid supplementation. The genes mutated in several mouse models of neural tube defects involve actin regulation, supporting the postulation that actin plays a key role in neurulation.

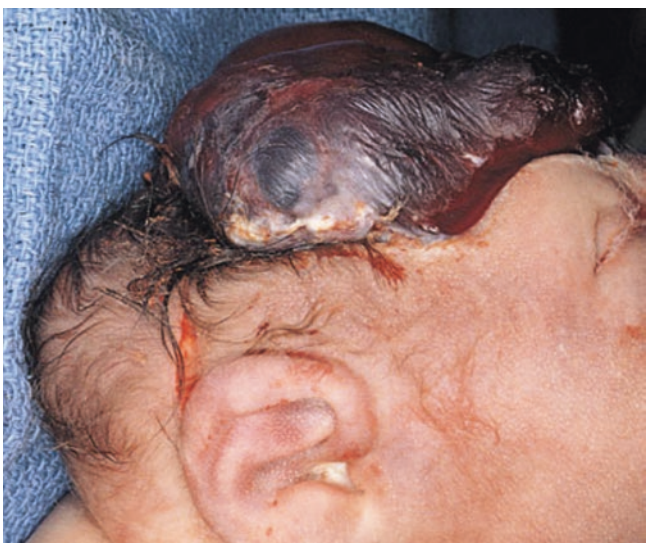

Fig. 2 Lateral view of an infant with anencephaly, showing lack of normal development of the brain, skull, and scalp

Encephalocele

An encephalocele (Fig. 3) is a neural tube defect in which there is extrusion of cranial contents through a bony defect in the skull. The pathogenesis is poorly understood but most likely involves defective development of the skull base. Encephaloceles can be located anywhere over the cranium, although most appear in the occipital (70–80%) or frontal locations. Parietal, nasal, and nasopharyngeal lesions may occur as well. Temporal lesions are the least common. Most defects are skin-covered, although some have only a thin, membranous cover that can rupture during delivery or with manipulation. The clinical consequences and prognosis are related directly to the contents of the encephalocele sac rather than the size of the defect. Approximately 20% of affected children are intellectual disability or have neurologic abnormalities. There is a high frequency of associated anomalies of the brain, such as neuronal migrational defects, absent corpus callosum, and hydrocephalus, and posterior fossa anomalies, including Dandy-Walker and Arnold-Chiari malformations. Extracranial anomalies occur more often with encephalocele than with other neural tube defects. All infants with encephaloceles should be examined carefully for additional anomalies, because a significant number of recognizable genetic syndromes include encephaloceles. The presence of a specific syndrome would alter the recurrence risk figures for future pregnancies. Encephaloceles occur in 1 in 5000 to 1 in 10,000 births. The recurrence risk for future pregnancies after the first affected child is about 6%. As with other neural tube defects, maternal use of folic acid before and during pregnancy may reduce the risk of recurrence.

Caudal Regression Sequence

Primary neurulation occurs during embryonic days 18–27 and involves the formation of the neural plate, neural tube, and spinal cord. Secondary neurulation occurs during embryonic days 28–48 and results in formation of the spinal cord below the lumbosacral junction. The paired somites, derived from mesoderm, develop along the spinal cord. The vertebral segments form from a portion of each somite. The caudal eminence, or tailbud, gives rise to the terminal spinal cord, the caudal notochord, vertebral segment S-2 through the last coccygeal segment, and parts of the hindgut and urogenital system. Thus, an insult to the caudal eminence may cause malformations in any of the structures normally derived from it, and might result in agenesis of sacral and coccygeal vertebrae and in lower gastrointestinal and urogenital anomalies.

Caudal regression sequence is a developmental field defect with absence or defects of structures derived from the embryonic caudal axis. Sacral agenesis and variable abnormalities of the lumbar vertebrae are commonly seen (Figs. 4, 5, and 6). Hypoplasia of the sacrum leads to flattening of the buttocks, shortening of the intergluteal cleft, or dimpling of the buttocks. There is frequently severe lack of growth in the caudal region. Sensory sparing is characteristic and suggests a relative preservation of neural crest cells. There may be abnormalities of the distal spinal cord with neurologic impairment. Other anomalies include imperforate anus or rectal agenesis, hypoplasia of the external genitalia, and renal anomalies or agenesis.

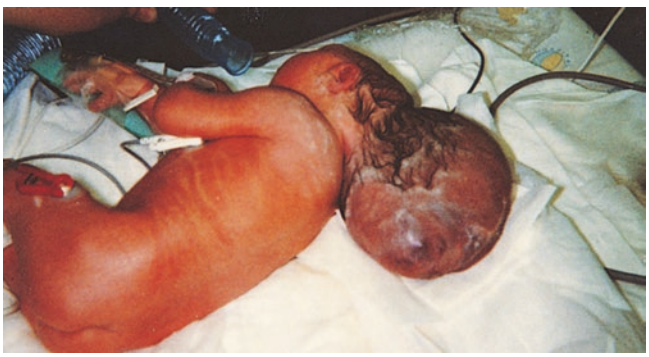

Fig. 3 Newborn infant with a massive occipital encephalocele. This infant had severe microcephaly with a bony defect in the occipital region of the skull; most of the brain tissue was contained within the encephalocele sac

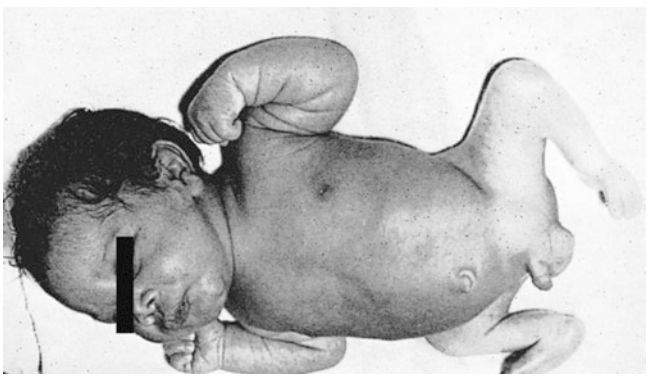

Fig. 4 Frontal view of an infant with caudal regression sequence showing a "frog leg" appearance of the lower extremities. There are abduction and flexion deformities of the hips as well as popliteal webs, *talipes equinovarus* deformity of the left foot, and *calcaneovalgus* deformity in the right foot. The upper body appears normal, but there is marked hypoplasia of the lower body

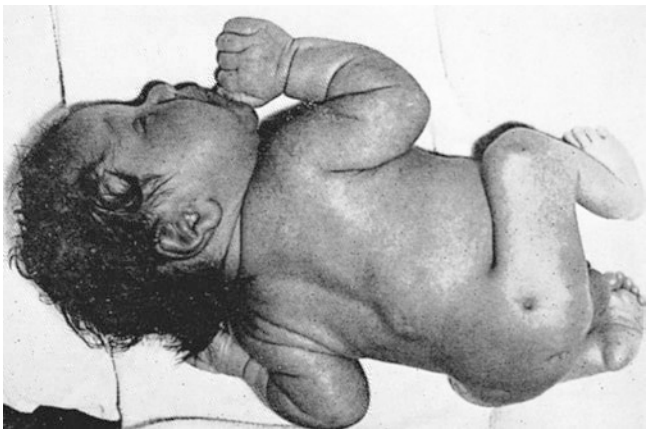

Fig. 5 Posterior view of the same infant as in Fig. 4, showing flat buttocks and sacral dimples, as well as a spinal projection of the lower back. Radiographic examination showed absence of the sacrum and lumbar vertebrae, fused iliac bones, and hypoplastic femurs. Hydronephrosis was present

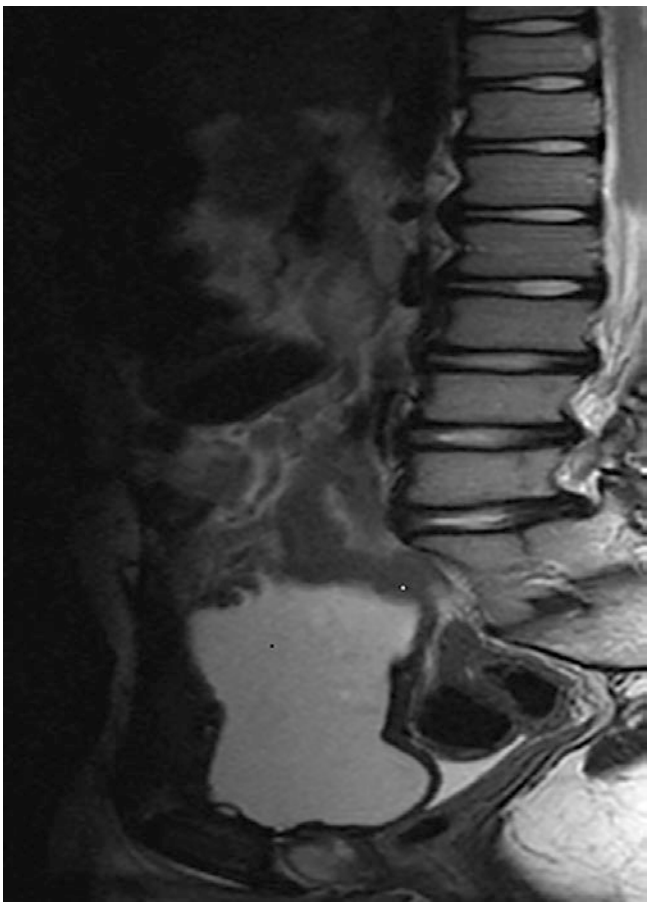

Fig. 6 Sagittal lumbosacral spine MRI image of the caudal regression sequence, showing hypoplastic sacral segments of spine (image courtesy of Dr. Alice Patton). Patients with this disorder may have associated small iliac wings, imperforate anus and hypoplasia of the external genitalia and lower extremities

Caudal regression has been previously grouped with *sirenomelia*, or *sympodia*, in which the lower extremities are fused, with posterior alignment of the knees and feet. These defects are now thought by some investigators to be pathogenetically different, with *sirenomelia* being caused by vitelline artery steal. Caudal regression sequence should also be distinguished from isolated sacral agenesis with or without spina bifida, which is probably a separate autosomal dominant condition.

Most cases of caudal regression sequence are sporadic with an unknown etiology, although there have been reports of Mendelian inheritance in some families. Maternal diabetes is thought to be responsible for at least 16% of cases, but only about 1% of diabetic mothers have offspring with caudal regression.

Holoprosencephaly Sequence

Holoprosencephaly (Fig. 7) occurs in approximately 1 in 13,000 live births, but the incidence is 50-fold greater in spontaneously aborted embryos. It lies at the severe end of the spectrum of disorders of prosencephalic development. Normally, neural tube closure is accomplished by embryonic day 28, followed by division into three distinct segments: From a rostral to caudal direction, these segments are termed the *prosencephalon*, *mesencephalon*, and *rhombencephalon*. The pre-notochordal mesoderm then induces the ventral aspect of the prosencephalon to differentiate into paired cerebral hemispheres, lateral ventricles, and the diencephalon, as well as the midline portion of the face. The induction

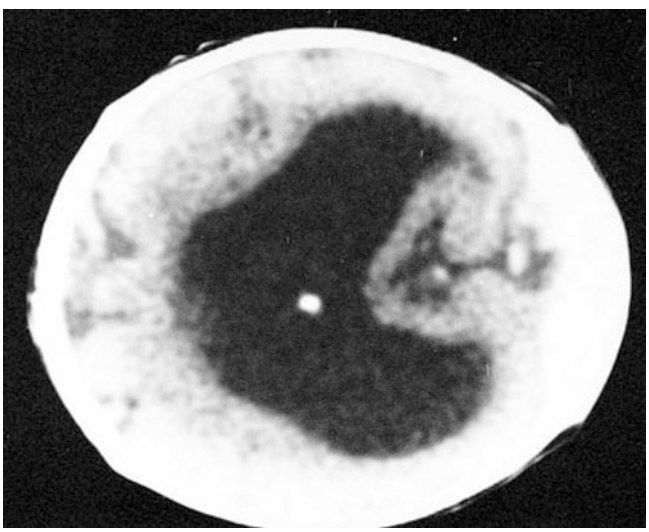

Fig. 7 CT image of the head of an infant who presented with developmental delay, displaying semilobar holoprosencephaly. Note the incomplete differentiation of the two lateral ventricles and absence of the septum pellucidum. The interhemispheric fissure is rudimentary in its anterior aspect but is better developed in the occipital regions

process consists of a group of cells secreting chemical signals that cause the surrounding tissue to change.

Holoprosencephaly is characterized by non-cleavage of the prosencephalon owing to failure of this normal inductive process. The timing of the insult is invariably prior to the 5th or 6th week of embryonic life. The failure of the telencephalon to cleave into the two cerebral hemispheres may be incomplete or complete. A single midline ventricle replaces the paired lateral ventricles. The cytoarchitecture of the cerebral cortex surrounding this single ventricle resembles that of the limbic cortex. Neuronal migration abnormalities are also visible. Holoprosencephaly is often associated with arhinencephaly (failure of the olfactory bulbs and tracts to develop and anosmia). The corpus callosum is also usually absent, as the presence of an interhemispheric fissure seems essential to the formation of the corpus callosum.

Most patients are microcephalic, but patients with macrocephaly from associated hydrocephalus have also been described. Associated facial anomalies include a single median incisor in the upper jaw, ocular hypotelorism, a single nostril, median cleft lip and palate, and a hypoplastic philtrum. Facial anomalies generally parallel the brain anomalies in severity. When associated with a single median eye, the disorder is termed *cyclopia*. Up to a third of the patients with holoprosencephaly show normal facial features, however. About three fourths of the patients have additional congenital anomalies involving the cardiovascular, genitourinary, or gastrointestinal system. Lesser degrees of abnormalities in prosencephalic development can lead to midline disorders such as agenesis of the corpus callosum (onset no later than 9–20 weeks of gestation), absence of the septum pellucidum, and septo-optic dysplasia (unilateral or bilateral optic nerve hypoplasia, absence of the septum pellucidum, hypothalamic dysfunction, and various degrees of cortical dysfunction in the form of seizures or intellectual deficit). Even milder forms of the holoprosencephaly sequence are characterized by subtle midfacial abnormalities such as single midline incisor or arhinencephaly (Fig. 8).

Antenatal diagnosis of the more severe forms can be established in the first and second trimesters using cranial ultrasound, which shows fusion of the cerebral hemispheres and thalami, and a single lateral ventricle. Cranial ultrasonography, CT, or MRI can establish the diagnosis after birth, with the MRI ideal for revealing the associated cortical migration abnormalities.

From conventional chromosomal studies, approximately half of the patients show normal karyotypes, whereas the remaining have trisomy 13–15, mosaic trisomy 13–15, trisomy 18, or deletion or ring abnormalities of chromosome 18 (Table 1). High-resolution banding and molecular studies may reveal chromosomal abnormalities not otherwise visualized using conventional cytogenetic methods cGH and exome sequencing. A mouse model of holoprosencephaly created by maternal exposure to alcohol during early pregnancy demonstrates a midline anterior neural plate deficiency that leads to positioning of the olfactory placodes too close to the midline and other secondary changes. Retinoic acid administration has also been implicated in the pathogenesis in some animal models of holoprosencephaly. Sporadic and autosomal dominant forms have been associated with mutations of the sonic hedgehog gene located on the 7q36 region, designated *HPE3*.

Table 1 Etiology of holoprosencephaly

Chromosomal anomalies
Mutations in the *ZIC-2* transcription factor gene
Chromosome 13: trisomy 13–15, trisomy 13–15 mosaicism, ring 13, deletion 13
Chromosome 18: trisomy 18, ring 18, deletion 18q
Chromosome 2, 3,7, and 21 deletions, trisomies
Triploidy 69, XX
Familial, without overt chromosomal anomalies
Autosomal dominant
Autosomal recessive
X-linked recessive
In association with normal karyotype and family history
Intrauterine ethanol exposure

Achondroplasia

Achondroplasia (Fig. 8), the most common skeletal dysplasia, occurs in approximately 1 of 16,000 to 1 of 35,000 newborns. It is characterized by significant macrocephaly, with head circumference well above normal for the age, a relatively normal trunk size, short stature, and rhizomelic shortening of the extremities with redundant folds of skin and soft tissue. Gross motor developmental milestones in infancy and early childhood are delayed because of hypotonia and short extremities. Individuals with achondroplasia are of normal intelligence, however, and can attain normal development within the limits of their short stature. Potential medical problems include an increased risk for respiratory disturbances, obstructive sleep apnea, and sudden infant death in infancy due to upper cervical spinal cord and medullary compression caused by narrowing of the foramen magnum. Mild enlargement of the ventricles frequently occurs with true megalencephaly, but frank hydrocephalus requiring treatment occurs in only about 5% of patients. Therefore, baseline MRI and serial brain ultrasonography until the patient is 1–2 years of age is recommended. Kyphosis, lordosis, and gibbus formation may develop. Lordosis and spinal stenosis with spinal cord compression symptoms may develop in adults with achondroplasia. Deformities of the lower extremities, such as genu valgum or varus, may require orthopedic intervention.

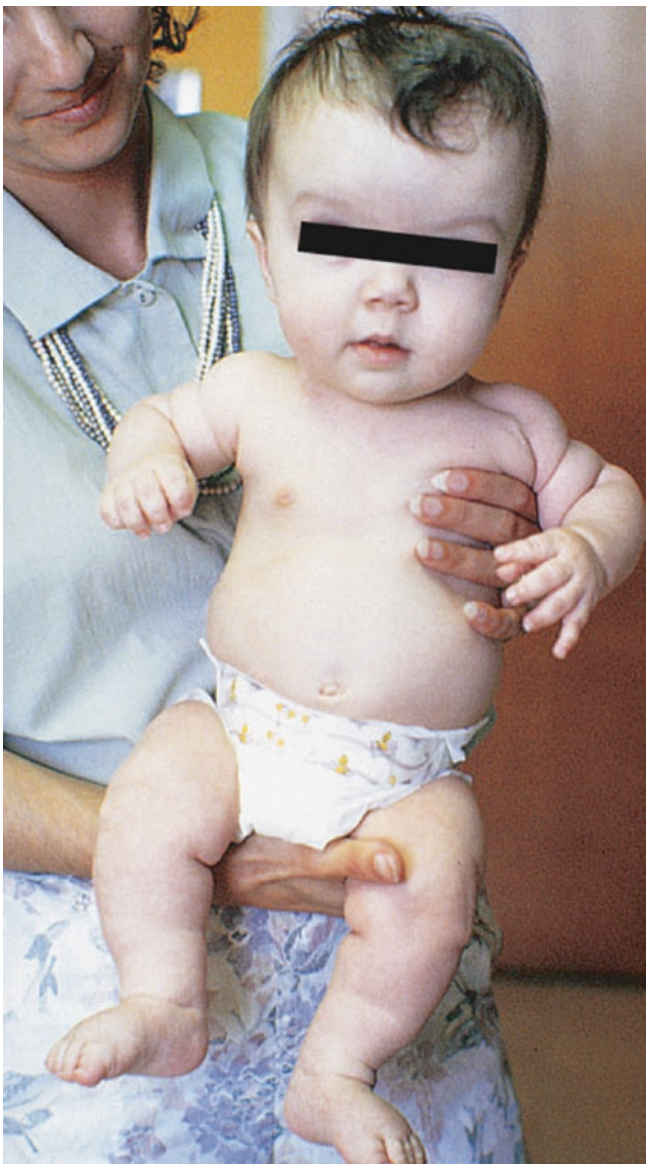

Fig. 8 Frontal view of a 9-month-old girl with typical achondroplasia

The phenotype is almost invariable from patient to patient, and the physical features are usually obvious at birth. Some cases can be detected by prenatal ultrasonography in the third trimester of pregnancy. The diagnosis is confirmed by radiographic examination. The interpedicular spaces narrow progressively in the lumbar spine, the sacrum is narrow and oriented horizontally, and the pelvis is short and broad. The vertebral bodies are concave posteriorly, and there may be anterior wedging of some vertebral bodies, especially at the thoracolumbar junction. The bones show rhizomelic shortening (proximal greater than distal), especially in the upper extremities. The fibula may be longer than normal at the distal end in relation to the tibia.

Achondroplasia is an autosomal dominant disorder with complete penetrance, although at least 80% of cases represent new mutations. The molecular genetic basis was discovered in 1994. Achondroplasia is caused by mutations in the gene for fibroblast growth factor receptor 3 (*FGFR3*), which is located on chromosome 4p16.3. More than 95% of all patients have either a G-to-A or a G-to-C point mutation in nucleotide 1138, which results in an amino acid change from glycine to arginine in the transmembrane portion of the molecule at position 380. Given that most cases are due to new mutations, nucleotide 1138 is the most highly mutable nucleotide currently known in the human genome. Several atypical cases of achondroplasia, and the related conditions of hypochondroplasia and thanatophoric dysplasia, have different mutations in the *FGFR3* gene.

Cortical Migrational Defects

Figure 9 illustrates the course of early neocortical layering and formation of the cortical plate. As shown in Fig. 9a, Layering involves the preplate zone, the marginal zone, and the subplate. The subplate is a precocious neuronal organization, complete with synaptic connections and long axons. The preplate and subplate neurons achieve a high level of morphologic maturity at early cortical stages. Subplate cells form local circuits and interconnections. The subplate receives the earliest afferent connections from outside the cortex, and its axons form the earliest efferent connections from the cortex to subcortical sites. If the subplate is destroyed, normal innervation and patterning of the cortex do not occur.

The cortical plate cells that are generated later collect between the marginal zone and subplate in an inside-out manner. In contrast, neuroblasts of the cortical plate are formed in proliferative regions lining the lumen of the neural tube, and postmitotic cells must migrate over long distances from these regions to the surface of the forebrain. Specialized radial glial cells seem essential to this migratory process. They are elongated glial cells that are anchored on both the pial surface (glia limitans) and the ventricular surfaces. As the cortical wall expands, the radial glia lengthen. These specialized glia provide radial scaffolding for the cortical plate neuroblasts, which appear to climb amoeba-like up the radial glia until reaching their correct position in the cortex. Neuroblasts secrete extracellular proteins such as astrotactin and reelin, which provide a receptor system for migration. Later, thalamic axons selectively extend in the subplate.

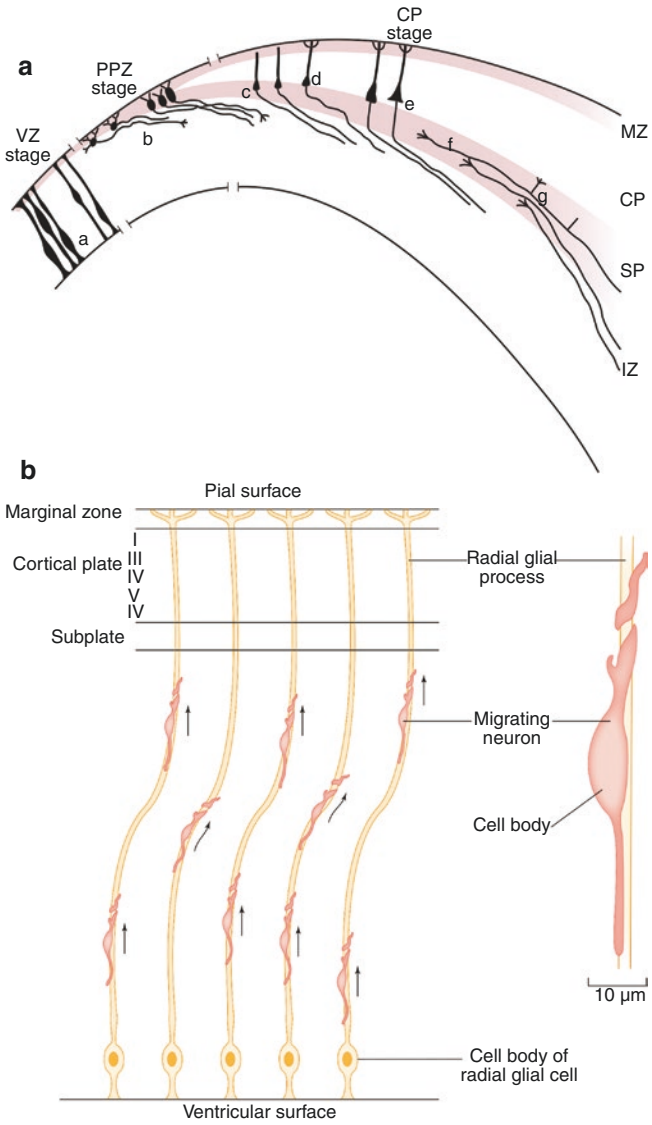

Fig. 9 Formation of early neocortical layering and the cortical plate. (**a**), The course of early neocortical layering. The preplate zone (PPZ), marginal zone (MZ), and subplate (SP) are highlighted by color. An idealized dorsolateral wall of the telencephalic vesicle is shown, and for convenience, three stages of early cortical development are represented. This compression is indicated by the *broken lines* at the pial (*upper*) and ventricular (*lower*) borders of the drawing. In the ventricular zone (VZ) stage, processes of dividing cells (a) and presumptive radial glia extend from pial to ventricular surfaces. In the PPZ stage (b), postmitotic neurons collect and extend axons. These cells later form the MZ and the subplate (c). The cortical plate (CP) cells that are generated later collect between the MZ and SP in an inside-out manner (d,e). Finally, thalamic axons selectively extend in the SP (f,g). (**b**)**,** Cortical plate formation. (From Rakic et al.; with permission)

In cortical plate formation (Fig. 9b), radial glia span the cortical wall. Neurons generated in the ventricular zone migrate up radial glia into position in the cortex. The cortical plate is formed in an inside-out manner. Layers IV and V are formed first, and more superficial neurons migrate past these to form the upper layers of the cortex. Cortical plate cells form layers II to VI of the cortex. The radial glia can be considered cells of the original columnar epithelium that became stretched as the cortical wall thickens.

Tubulin genes seem to play a major role in the pathogenesis of malformations of cortical development. They are expressed in post-mitotic neurons, and influence neuronal migration and axonal guidance. They encode for dimeric proteins, α and β tubulin, which are a major component of microtubules. Mutations in tubulin-associated genes have been implicated in the pathogenesis of several brain malformations, such as lissencephaly, micropolygyria, schizencephaly, and agenesis of the corpus callosum. Lately, targeted sequencing using a panel of known and candidate genes associated with brain malformations has successfully identified somatic cell mutations in approximately 17% of patients with brain malformations. The genes identified using this approach have included *DCX* and *LIS1* in patients with double cortex, *FLNA* in patients with nodular periventricular heterotopia, and *TUBB2B* in patients with pachygyria.

Lissencephaly

Lissencephaly (Fig. 10) implies a smooth brain and represents a failure to form normal convolutions, resulting in a smooth cortical surface. Cortical development proceeds to cleavage into two hemispheres and the formation of the sylvian fissure, but normal migration fails. In all forms of lissencephaly, there is an outer layer that may represent the preplate, but the remaining neurons do not form the normal six-layered cortex and have been arrested or stopped during migration. Often the lissencephalic cortex has large, simple gyri called pachygyria. Lissencephaly may be associated with focal areas of pachygyria. Classic lissencephaly is most commonly from a mutation of one of three genes: *Lis1* (also called *PAFAH1B1*), *DCX*, and *TUBA1A*. The gene *ARX* causes lissencephaly with genital malformations.

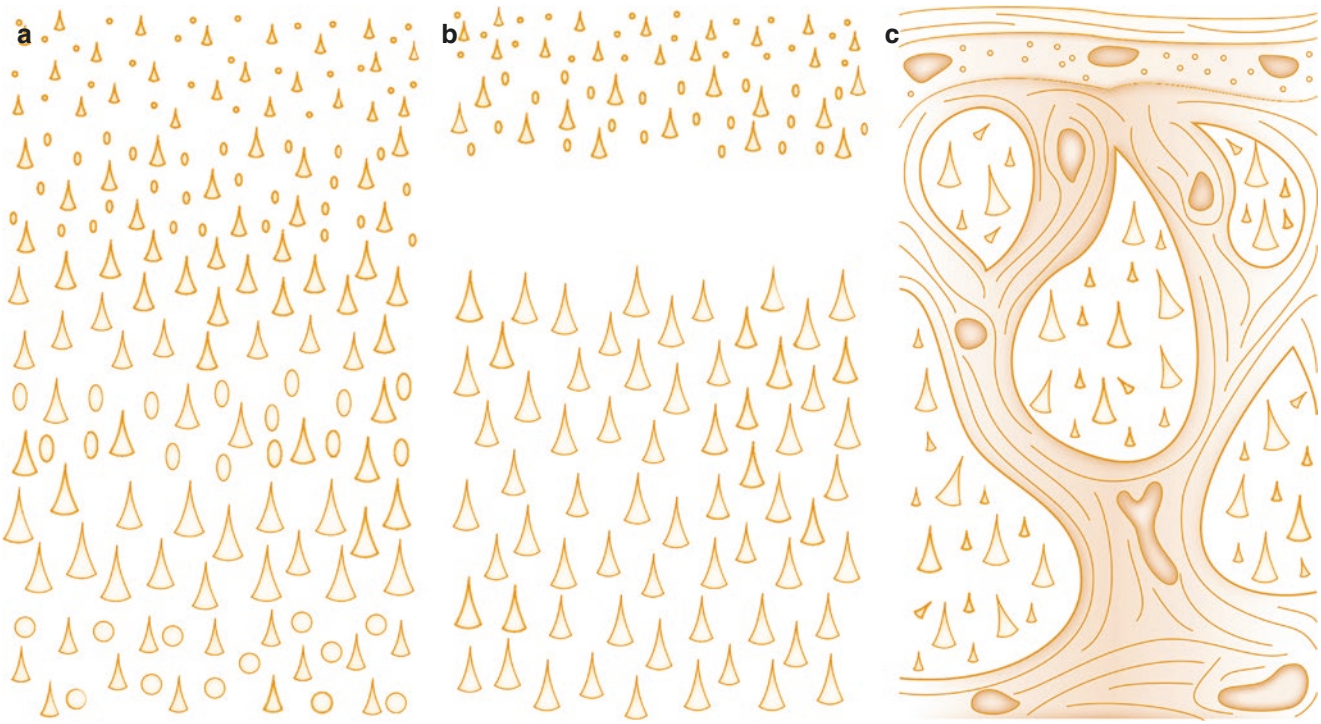

Fig. 10 A normal cerebral cortex compared with a classic lissencephalic cerebral cortex. (**a**) Normal six-layer cortex. (**b**) Classic lissencephaly with a four layer cortex: a thick, deep layer of cells arrested in migration; a relatively cell-free layer; a layer of disorganized early migrating cells; and a molecular layer. (**c**) Type II lissencephaly: thickened meninges obscure the molecular layer in some places. Gliomesenchymal bundles isolate neuronal heterotopias. (Adapted from Aicardi; with permission)

Several classification systems have been used for lissencephaly. In the most commonly used system, lissencephaly is classed as type I or classic lissencephaly; type II, or cobblestone lissencephaly; and sporadic lissencephaly. The different forms of lissencephaly are caused by separate genetic mutations and show differences in severity and microscopic anatomy.

Classic Lissencephaly

Type I lissencephaly (classic lissencephaly) shows thickened simple cortex (Fig. 11). Much of the cortical surface is smooth and agyric. With *Lis1* mutation, the posterior brain is most affected. The extent of the agyria varies. Many brains have pachygyria, particularly on the inferior and frontal surfaces of the cortex. Because of the association with pachygyria, some authorities have called type I lissencephaly the *agyria-pachygyria complex*. When the sylvian fissure has formed, transverse sections give a "figure 8" appearance to the cortex. This characteristic shape of the telencephalon may be seen on either CT or MRI. The ventricles keep their fetal shape and thus appear enlarged, with occipital dilatation or colpocephaly. The hippocampus is small and may be simple. Often the brainstem is hypoplastic, with heterotopia in the olivary nuclei. Usually there is a corpus callosum, although its body may be short or hypoplastic. Myelination of white matter and the corpus callosum occurs at developmentally appropriate times. Heterotopia may appear along the ventricle, within the band of white matter.

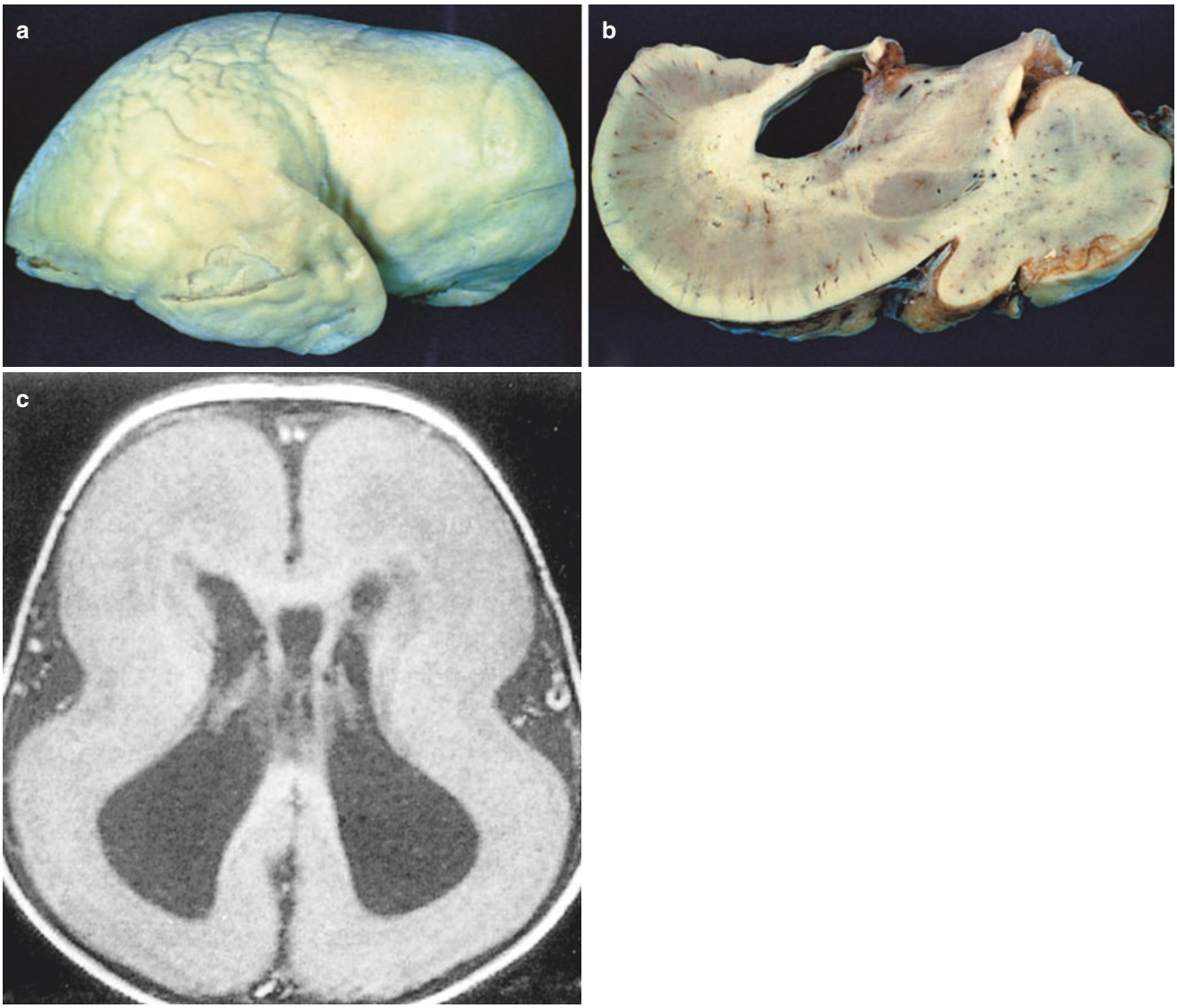

Fig. 11 Thickened simple cortex showing type I lissencephaly (classic lissencephaly). (**a** and **b**) On gross inspection, much of the cortical surface is smooth and agyric. (**c**) T1-weighted MRI of type I lissencephaly

Mutations of both the *Lis1* gene and nearby *YWHAE* gene produce Miller-Dieker syndrome (Fig. 12). Phenotypic features include an upturned nose, micrognathia, protuberant upper lip with thin vermillion border, and bitemporal hollowing. At birth, the head circumference may be normal, but as the growth rate falls off, microcephaly develops. Most affected individuals are hypotonic, severely developmentally delayed, and have intractable epilepsy (including infantile spasms) and feeding difficulties. Survival is often short, with many children dying by 5–10 years of age. Classic lissencephaly occurs in Miller-Dieker syndrome. Not all classic lissencephaly patients have Miller-Dieker syndrome, although affected individuals usually have some of the phenotypic features.

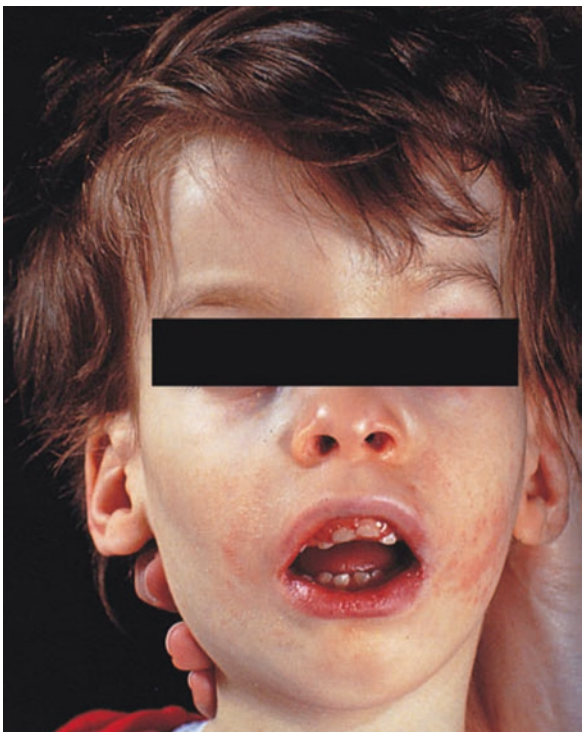

Fig. 12 The facial features of Miller-Dieker syndrome

Initially described by Miller in 1963 and Dieker in 1969, type I lissencephaly was at first attributed to a familial autosomal recessive disorder with occasional sporadic or isolated cases. High-resolution chromosome banding techniques demonstrated deletion of band 17p13 in Miller-Dieker syndrome. Development of fluorescence in situ hybridization (FISH) probes into the lissencephaly region demonstrated deletions in the 17p13.3 region in the majority of both Miller-Dieker patients and patients with isolated lissencephaly (Fig. 13). The *LIS1* gene has been localized to this region. Most, if not all, familial cases are secondary to balanced translocations in one of the parents. Analysis of parental chromosomes is necessary, and will assist in predicting the likelihood of recurrence in a given family. Additional types of lissencephaly include X-linked lissencephaly related to mutations in the doublecortin (*DCX*) gene, and X-linked lissencephaly with absent corpus callosum and abnormal genitalia, which is related to mutations in the *ARX* gene.

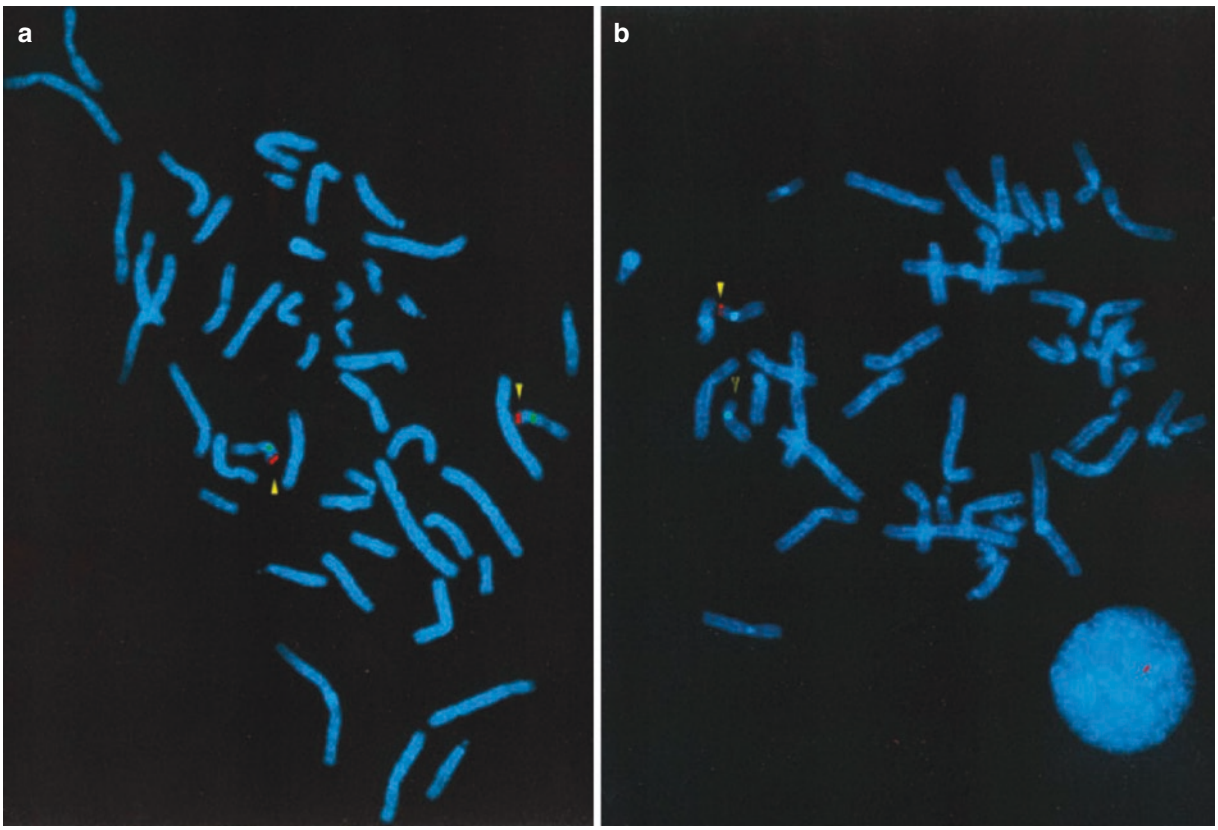

Fig. 13 Fluorescence in situ hybridization (FISH) probes of chromosomes of a normal individual and a patient with type I lissencephaly. (**a**) Chromosomes in metaphase are counterstained with a chromosome 17–specific centromeric α satellite probe (*green*). A cosmid probe from within the smallest deletion interval for lissencephaly is detected with rhodamine (*red*). In a normal individual, the cosmid probe shows two positive signals on each chromosome 17 (*yellow filled arrowheads*). (**b**) In a lissencephaly patient with submicroscopic deletion, there is one normal chromosome 17 (*filled arrowhead*), and the other homologue shows no hybridization to the cosmid probe (*open arrowhead*). The failure of labeling in the lissencephaly patient indicates a deletion in the 17p13 region

X-Linked Lissencephaly and Subcortical Band Heterotopias

X-linked lissencephaly is a type of lissencephaly syndrome related to mutations in the doublecortin (*DCX*) gene, which is localized on Xq21-24. The gene contains a tyrosine kinase phosphorylation site which is important for signal transduction, and consequently, neuroblast migration. Females with this condition usually manifest subcortical band heterotopias, whereas males show lissencephaly. Females may be asymptomatic, or manifest epilepsy. Males have a more severe phenotype, with both mental retardation and epilepsy.

X-linked lissencephaly and subcortical band heterotopia (also called double cortex) (Fig. 14) are caused by a mutation of the doublecortin gene (*DCX*) on the X chromosome. Hemizygous males have a gradient of severity ranging from pachygyria to classic lissencephaly, whereas females express band heterotopia. The anterior brain is most affected with *DCX* mutations. Females may be asymptomatic but frequently have severe seizures and may be mentally retarded. Recurrence risk in carriers is high, with half of boys having lissencephaly and half of girls having a double cortex.

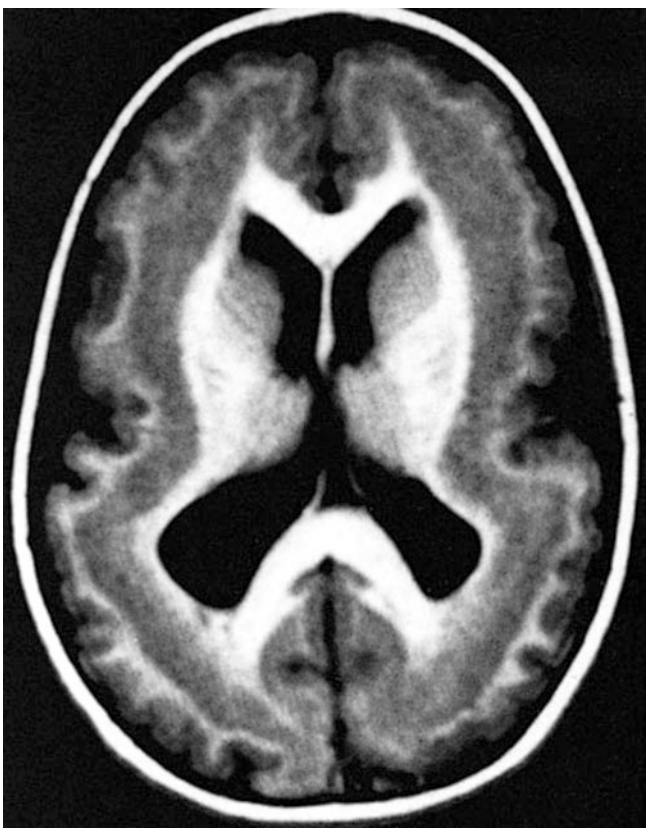

Fig. 14 T1-weighted MRI of a double cortex (subcortical band heterotopia)

Cobblestone Lissencephaly

Lissencephaly type II is now called cobblestone lissencephaly or cobblestone complex (Fig. 15). Cobblestone lissencephaly is a continuum of recessive disorders involving brain, eye, and muscle including Walker-Warburg syndrome (WWS), Muscle-Eye-Brain disease, and Fukuyama muscular and cerebral dystrophy. These disorders are caused by mutations affecting glycosylation of α-dystroglycan. This in turn disrupts the interaction of the radial glia and the outermost pial-glial membrane, called the glia limitans. Migrating precursor cells escape the wall of the brain and form clumps in the arachnoid space. The genes most commonly associated with cobblestone lissencephaly are *POMT1*, *FKTN*, and *LARGE*.

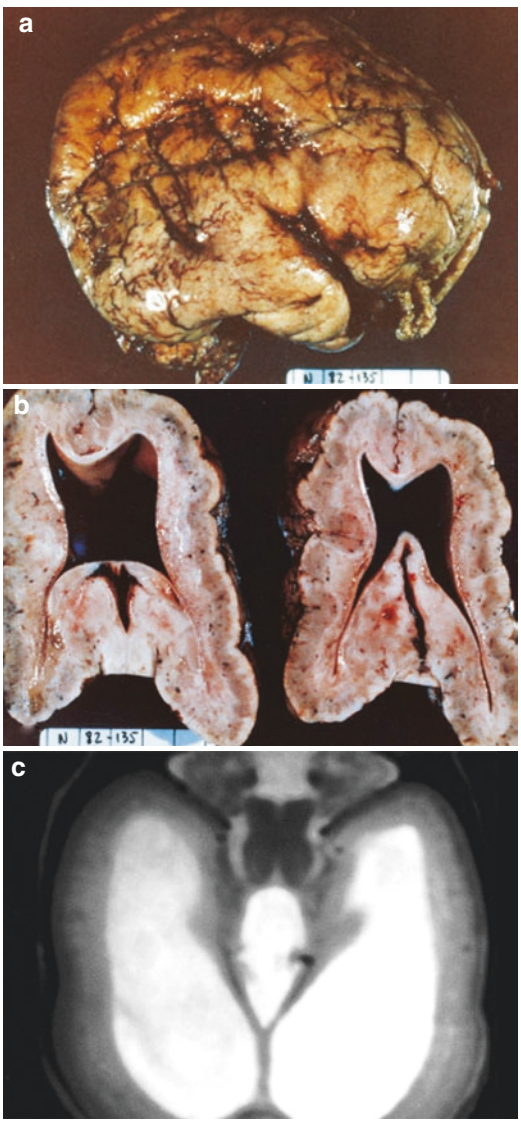

Fig. 15 Pathologic specimen and MRI showing lissencephaly type II, now called cobblestone lissencephaly. (**a** and **b**) The cortex has an irregular surface and thickened meninges. (**c**) MRI scan of Walker-Warburg syndrome (WWS). (Courtesy of William Dobyns, University of Washington)

The most severe form is Walker-Warburg syndrome (WWS). The typical presentation is severe, with macrocephaly secondary to hydrocephalus, weakness, and seizures, with death expected in the first years of life. Although the cortex has areas of agyria, other pathologic changes clearly separate this from other types of lissencephaly. Four abnormalities are required for the diagnosis of this disorder: lissencephaly, cerebellar malformation, retinal malformation, and congenital muscular dystrophy. The facial appearance varies but usually includes a high forehead and facial weakness. Ocular abnormalities may include microphthalmia, cataracts, congenital glaucoma, coloboma, and optic nerve hypoplasia. Retinal dysplasia and detachments occur in all patients. Unlike classic lissencephaly, areas of polymicrogyria and pachygyria may "cobblestone" the surface of the brain. The cerebella are small and aplastic, the vermi absent or hypoplastic, and the folia small with microgyria and rosette formations. Agenesis of the corpus callosum is common. Neuroimaging of type II lissencephaly demonstrates lissencephaly, a varying degree of hydrocephalus, and a Dandy-Walker malformation (Fig. 15c). Posterior encephaloceles are common. The meninges are thickened and appear inflamed. Leptomeningeal neuronal and glial heterotopia may partly obstruct the subarachnoid space and cause fusion of the two cerebral hemispheres. Whether ventricular dilatation is secondary to meningeal adhesion, the Dandy-Walker malformation, or aqueductal stenosis is unclear.

Pachygyria

Pachygyria (Fig. 16) refers to a cerebral cortex developing overly large gyri, instead of the normal development of several smaller gyri. Usually diagnosed on MRI, pachygyria may be generalized across the cortex or lateralized or focal over one hemisphere. Most generalized pachygyria is caused by milder expressions of the same genes that cause type I lissencephaly. The location of the pachygyria depends on the underlying cause. For instance, *Lis 1* deletions are more severe posteriorly, whereas *DCX* mutations are most severe anteriorly. A single photon emission CT (SPECT) scan may show decreased perfusion in the affected area. SPECT scanning may detect subtle areas of cortical malformation and is performed in many medical centers prior to epilepsy surgery.

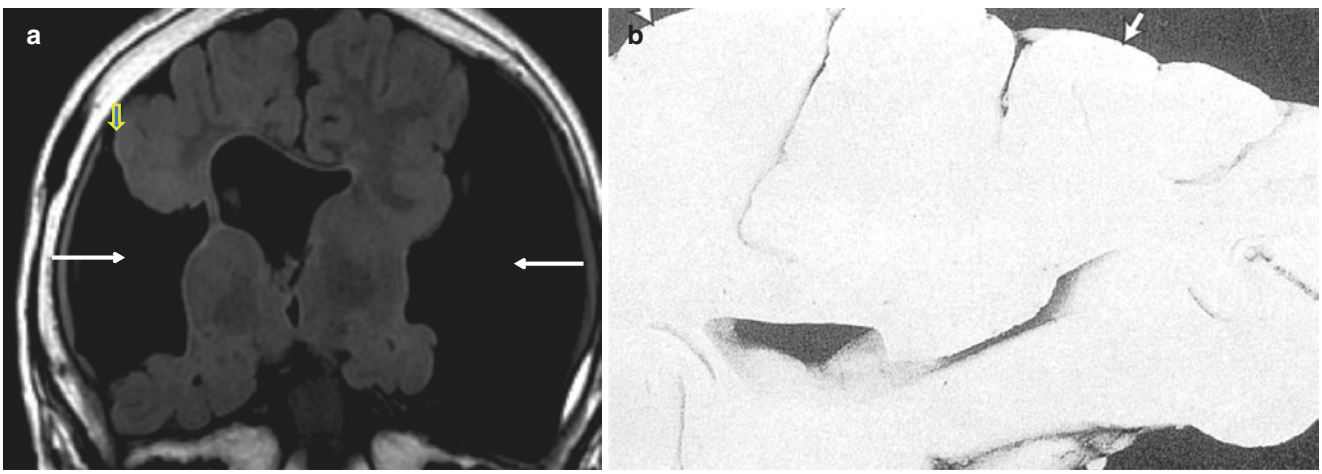

Fig. 16 Neuroimages and a gross specimen showing pachygyria. (**a**) Coronal T1 weighted MRI image showing bilateral open-lip schizencephaly (*large white arrows*) in association with pachygyria (*yellow arrow*). (**b**) Gross specimen of the parieto-occipital region of the brain demonstrating pachygyria (*arrow*) (From Byrd et al., with permission)

Polymicrogyria

Polymicrogyria (Fig. 17) may be focal, bilateral, or generalized across the cortex. Polymicrogyria is linked to disruptions in cortical genesis after migration has begun. Its diverse etiologies include congenital infection, hypoxia with laminar necrosis, and genetic causes. Over 30 genes have been linked to polymicrogyria, most in the tubulin family. Four-layer polymicrogyria is attributed to laminar necrosis of layers V and VII. One-layer microgyria is generally disorganized and is attributed to cell loss in weeks 15–17 of pregnancy.

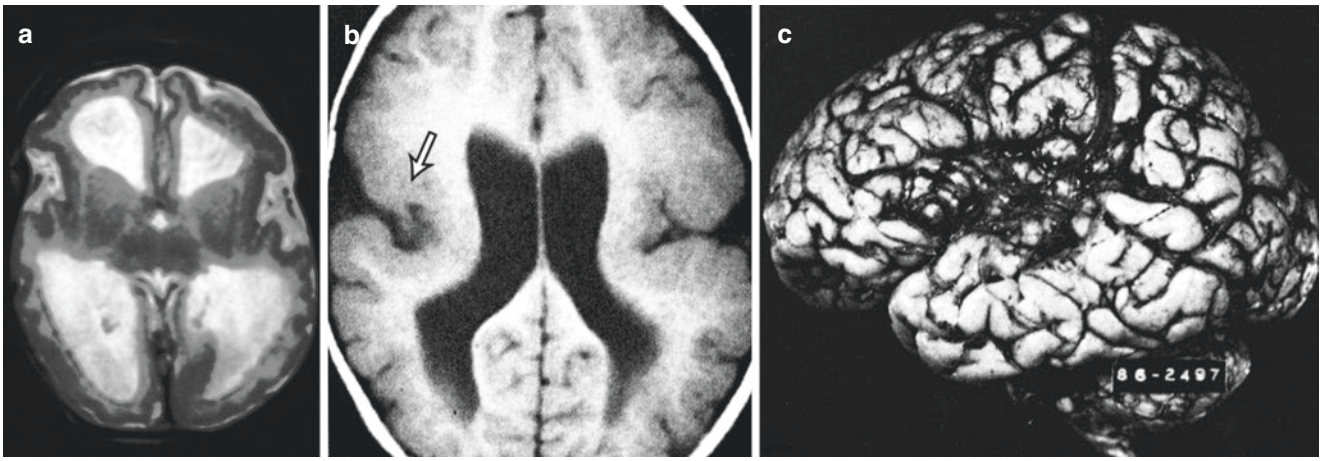

Fig. 17 MRI scans showing polymicrogyria. (**a**) T2-weighted MRI. (**b**) T1-weighted MRI of perisylvian polymicrogyria (*arrow*). (**c**) Pathologic specimen of perisylvian polymicrogyria. (**a** and **b**, Courtesy of William Dobyns, University of Washington; **c**, From Becker et al., with permission)

Superficially, the MRI in Fig. 17 appears to show pachygyria and ventriculomegaly, but closer inspection of the surface reveals polymicrogyria. The nubby surface appearance helps to distinguish polymicrogyria from pachygyria. Generalized polymicrogyria has been linked to congenital cytomegalovirus infection but may have a genetic or metabolic cause. Perisylvian polymicrogyria (Fig. 17b, c) was recognized after neuroimaging became a common procedure in cases of epilepsy. Perisylvian polymicrogyria and other symmetric polymicrogyrias have been linked to multiple genes and can be both dominant and recessive disorders. Symmetric polymicrogyria appears less commonly in the frontal and parietal lobes. Of note, closed-lip schizencephaly (discussed below) is considered a type of polymicrogyria.

Porencephaly

Destructive lesions within the vascular distribution of a blood vessel underlie porencephaly (Fig. 18). Lesions are more common in twin pregnancies or following maternal hypotension, both of which increase the probability of vascular events occurring in the fetus. The gestational timing of the vascular event determines the appearance of the lesion. Infarction after the period of neuronal migration results in tissue loss and cavitation, frequently with a membrane, and the cyst may be under tension. As depicted in Fig. 18b, the anatomy of the circle of Willis is disrupted, and the left middle cerebral artery is ablated.

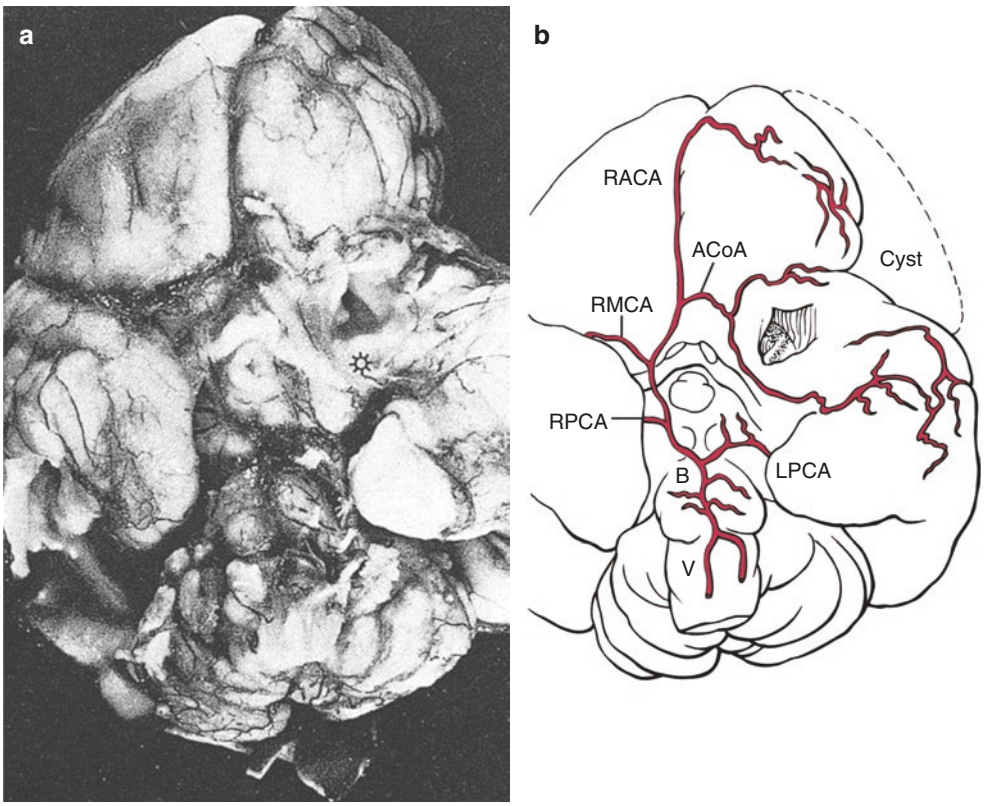

Fig. 18 Porencephaly. (**a**) Ventral surface of the brain of a child who died of multiple congenital defects and porencephaly 1 h after birth. In this specimen, a defect or cleft in the left frontal lobe extends into the ventricular space (*asterisk*). The cystic membrane was destroyed when the brain was removed. (**b**) Drawing of the ventral surface of the brain, illustrating the original cystic membrane. *ACoA* anterior communicating artery, *B* basilar artery, *LPCA* left posterior cerebral artery, *RACA* right anterior cerebral artery, *RMCA* right middle cerebral artery, *RPCA* right posterior cerebral artery, *V* vertebrae. (From Stewart, with permission)

Schizencephaly

Destructive events occurring within the period of neuronal migration may cause schizencephaly (Fig. 19). Loss of the cortical wall causes a cleft, and if the ependymal lining of the ventricle is damaged, the defect will communicate with the ventricular system. Most clefts occur in the distribution of the middle cerebral artery. However, not all cases of schizencephaly are secondary to vascular events. Germline mutations of the homeobox gene *EMX2* produce a severe form of open-lip schizencephaly. Schizencephaly is associated with focal or generalized epilepsy. The lesion may be overlooked on CT and is best seen with MRI. Clefts in schizencephaly extend from the cortical surface to the ventricle and are lined with cortex. Mental retardation occurs in 15% of unilateral lesions and approaches 90% in bilateral lesions.

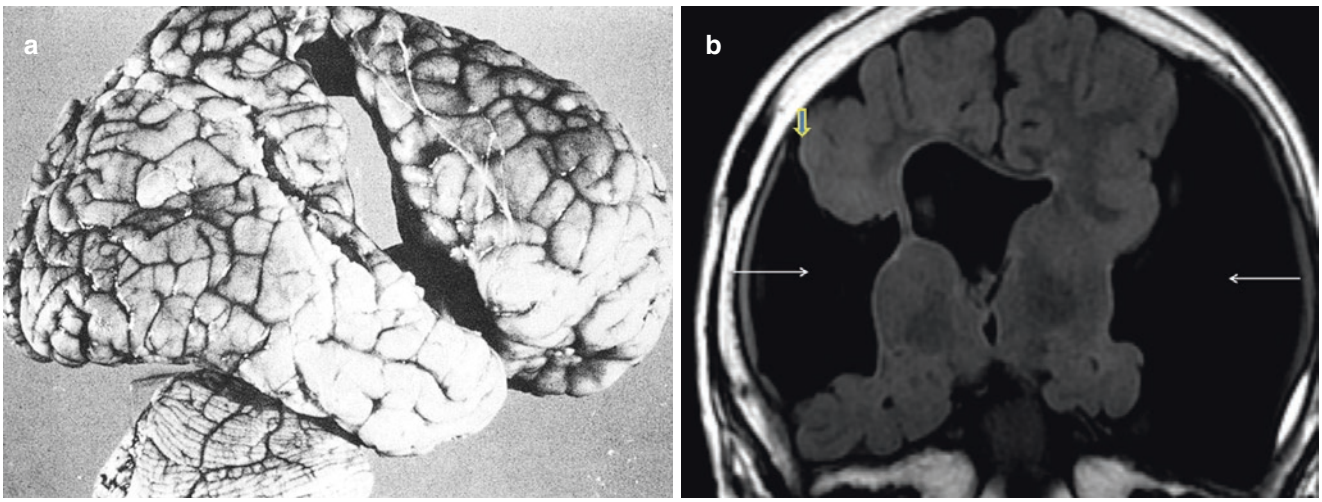

Fig. 19 Schizencephaly. (**a**) Pathologic specimen showing bilateral, large open-lip schizencephaly. (**b**) T1-weighted MRI of a unilateral closed-lip schizencephaly in a 5-year-old child. The cleft is lined with cortex that shows polymicrogyria. This child was mildly developmentally delayed and seizure-free. (**a**, From Norman and Ludwin, with permission)

Focal Cortical Dysplasia

Focal cortical dysplasia (FCD) is a defined subgroup of malformations of cortical development. FCD refers to a spectrum of abnormalities involving the laminar structure of the cortex. The cytopathological features include dyslamination with or without dysmorphic neurons and balloon cells. The main clinical manifestation of FCD is epilepsy. Seizures typically start during early childhood with high seizure burden, and may remain refractory to medical management, but epilepsy in FCD is potentially amenable to surgical intervention. In epilepsy surgery series, FCD accounts for about 20–25% of patients. It is the most common histopathology found in the pediatric epilepsy surgery cohort and the third most frequent cause identified in adult epilepsy surgery patients. About 60% of patients with cortical dysplasia are seizure-free after surgery, with the best predictor of seizure-free outcome dependent on extent of resection of MRI lesion and epileptogenic zones. Neurophysiologic investigations for presurgical planning show complex epileptogenic networks that may include noncontiguous regions. The MRI visible area of cortical abnormality is a marker of the epileptogenic zone rather than the entirety of the epileptogenic substrate. Removal of the epileptogenic zone including the ictal onset zone (where seizures are initiated) and the epileptic lesion may improve the outcome of lesionectomy. Surgical planning also requires attention to functional representation around the FCD. Localization of function based on anatomic landmarks is not reliable; individual variations are present in which atypical representation or relocation of function could be present around the radiographically evident FCD.

The 2011 International League against Epilepsy (ILAE) classification (Table 2) updated the 2004 Palmini et al. classification. ILAE FCD type I and type II are isolated cortical dysplasia, whereas type III is dysplasia associated with other epileptogenic lesions. FCD type I is malformation with disrupted cortical lamination. Dysmorphic neurons are a hallmark of type IIA, whereas type IIB is specified by the presence of dysmorphic neurons and balloon cells (Fig. 20). Balloon cells can occur in any cortical location; they have a large cell body, with abundant eosinophilic cytoplasm on hematoxylin and eosin staining and an eccentric nucleus; multiple nuclei may be present. FCD not otherwise specified includes cases associated with a clinically suspected principal lesion that is not available for histopathological examination. FCD has many probable etiologies. FCD type II is now classified as a malformation due to abnormal proliferation. FCD types I and III are classified as malformations secondary to abnormal postmigrational development because they can result from prenatal and perinatal insults.

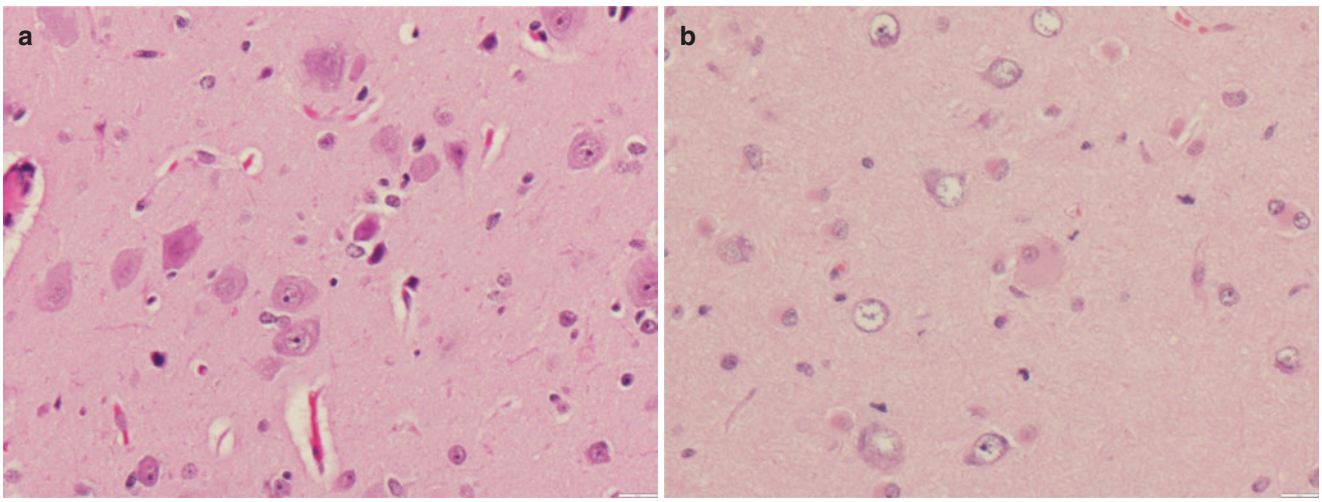

Fig. 20 Focal cortical dysplasia (FCD). (**a**) Type IIA, with dysmorphic neurons with enlarged nuclei (H&E). Dysmorphic neurons present with enlarged cell body and nucleus, malorientation, abnormally distributed intracellular Nissl substances, and cytoplasmic accumulation of neurofilament proteins. (**b**) Type IIB balloon cells (H&E)

Table 2 Comparison of Palmini and ILAE FCD classification

Palmini et al. (2004)		ILAE (2011)	
Type		Type	
Mild malformation of cortical development (mMCD)			
mMCD type I	Ectopically placed neurons in or adjacent to layer I		
mMCD type II	Microscopic neuronal heterotopia outside layer I		
Focal cortical dysplasia (FCD)			
FCD type IA	Isolated architectural abnormalities (dyslamination, ± other abnormalities of mMCD)	FCD type IA	Abnormal radial cortical lamination
FCD type IB	Architectural abnormalities, plus giant or immature but not *dysmorphic* neurons	FCD type IB	Abnormal tangential lamination
FCD type IIA	Architectural abnormalities with dysmorphic neurons but without balloon cells	FCD type IC	Abnormal radial and tangential lamination
FCD type IIB	Architectural abnormalities with dysmorphic neurons with dysmorphic and balloon cells	FCD type IIA	Cortical lamination abnormalities with dysmorphic neurons
		FCD type IIB	Cortical lamination abnormalities with dysmorphic neurons and balloon cells
		FCD type IIIA	FCD associated with hippocampal sclerosis
		FCD type IIIB	FCD adjacent to a glial glioneuronal tumor
		FCD type IIIC	FCD adjacent to a vascular malformation
		FCD type IIID	FCD adjacent to another lesion acquired during early life

Adapted from Blümcke et al.

The precise mechanisms of the epileptogenicity of FCD remain to be elucidated. The imbalance of neuronal hyperexcitability may be related to disrupted ionic homeostasis from aberrant expression of neurotransmitter receptors and ion channels. Activation of mTOR signaling has been identified in an FCD type IIB surgical specimen. In animal models, the epileptic phenotype has been shown to be rescued with rapamycin, an inhibitor of mTOR complex 1, highlighting the potential implications of mTOR for epileptogenesis.

The MRI findings of FCD include cortical thickening, abnormal gyration pattern, loss of gray-white differentiation, and increased T2 signal in the subcortical white matter. FCD type II is seen more often in extratemporal regions, with preference for the frontal lobes (Fig. 21). A common MRI finding in FCD type IIB is the transmantle sign: subcortical white matter hyperintensity extending from cortical thickening in the overlying cortex and bottom of the sulcus dysplasia to the lateral ventricle. FCD type IIB has been associated with favorable seizure control after surgical resection, but it is not known whether the favorable outcome may be related to lower epileptogenicity or easier anatomic recognition of the epileptogenic lesion.

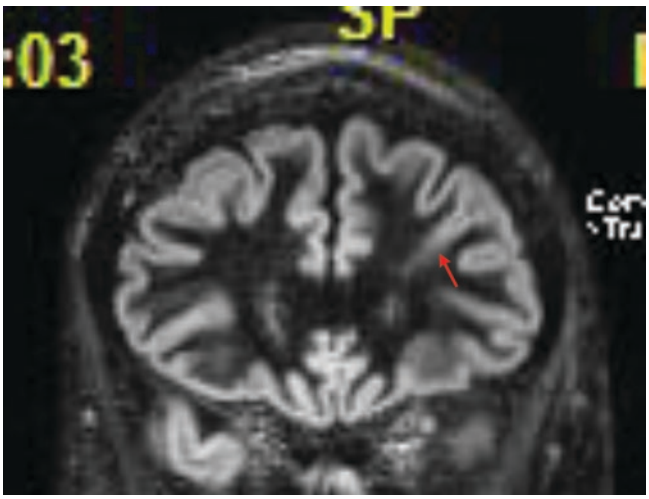

Fig. 21 Double inversion recovery reformatted image from a 12-year-old boy with medically refractory focal epilepsy since age 7 years. The left frontal lobe shows FCD with blurring of the *gray-white* interface and increased transmantle signal in adjacent white matter (*arrow*). Histopathology of a left frontal cortical resection showed FCD IIB

About one third to one half of patients with pathology-confirmed FCD have normal brain MRI (Fig. 22). About 90% of patients with FCD type II have MRI abnormalities, compared with only 30% of patients with FCD type I. In MRI-negative epilepsy, FDG-PET shows corresponding areas of hypometabolism in up to 90% of patients later found to have FCD. Subtraction ictal SPECT co-registered to MRI is nonspecific for FCD, but has been positive in 80% of histopathology-confirmed cases. Voxel-based morphometry has been shown to have higher sensitivity than conventional visual analysis. Diffusion tensor imaging and EEG-fMRI has shown some promise in providing additional localizing information in MRI-negative cases.

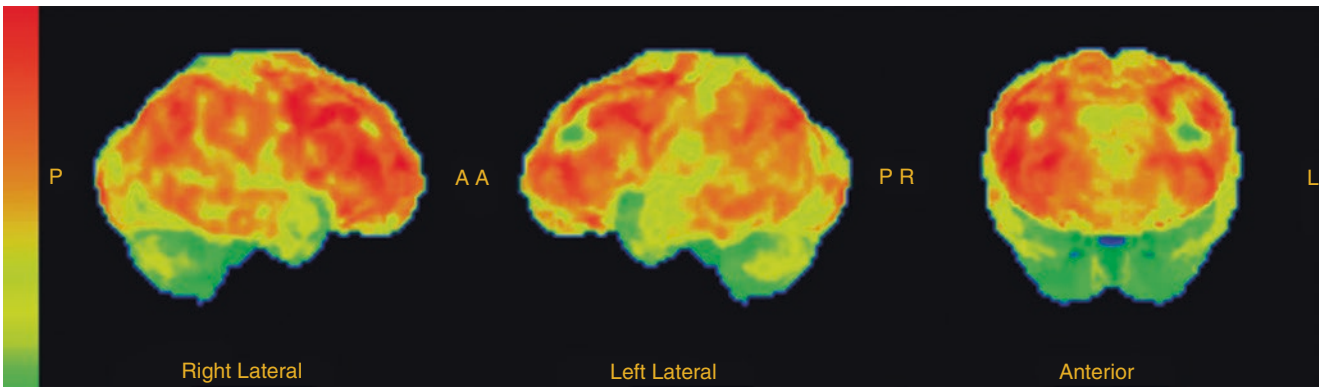

Fig. 22 3 T MRI of the brain was normal in this 15-year-old male with a history of medically refractory frontal lobe epilepsy since age 5 years. FDG-PET showed hypometabolism in the left frontal lobe. Histopathology from a left frontal cortical resection showed FCD type IIA

Hydranencephaly

Hydranencephaly (Fig. 23) is an encephaloclastic disorder in which nearly the entire telencephalon is destroyed, presumably by disruption of bilateral carotid arterial flow. The vertebrobasilar circulation is preserved, which is reflected in the relative preservation of the brainstem and cerebellum, as well as occasional portions of the occipital and inferior temporal cortex. This is a disorder of destruction of previously formed tissue, with onset early enough in gestation to produce cavitation but with a minimum of reactive gliosis. The hemispheres are replaced by fluid-filled cavities lined with a thin membrane that abuts the dura mater. The etiology of the vascular disruption varies and includes infections with cytomegalovirus, syphilis, toxoplasmosis, and influenza. Attempted abortions, radiation exposure, and, rarely, embryonal tumors of the hemispheres have also been associated with the disorder.

Clinically, the child may appear normal if the hypothalamus is intact, and the head size and shape may be normal at birth but grow rapidly thereafter. Lethargy and extreme thermoregulatory instability may be observed in those with impaired diencephalic function. Transillumination of the skull demonstrates the large fluid sacs with small overlying vessels. The patients have a poor prognosis, with anticipated survival of only a few years. They often lack normal diurnal sleep-wake rhythm organization, which complicates their care. Radiographically, the skull and falx appear normally formed, but the hemispheres are replaced by large cysts. Electrophysiologically, cortical evoked potentials are absent and the electroencephalogram (EEG) is flat, or nearly so. Brainstem responses are generally intact, however.

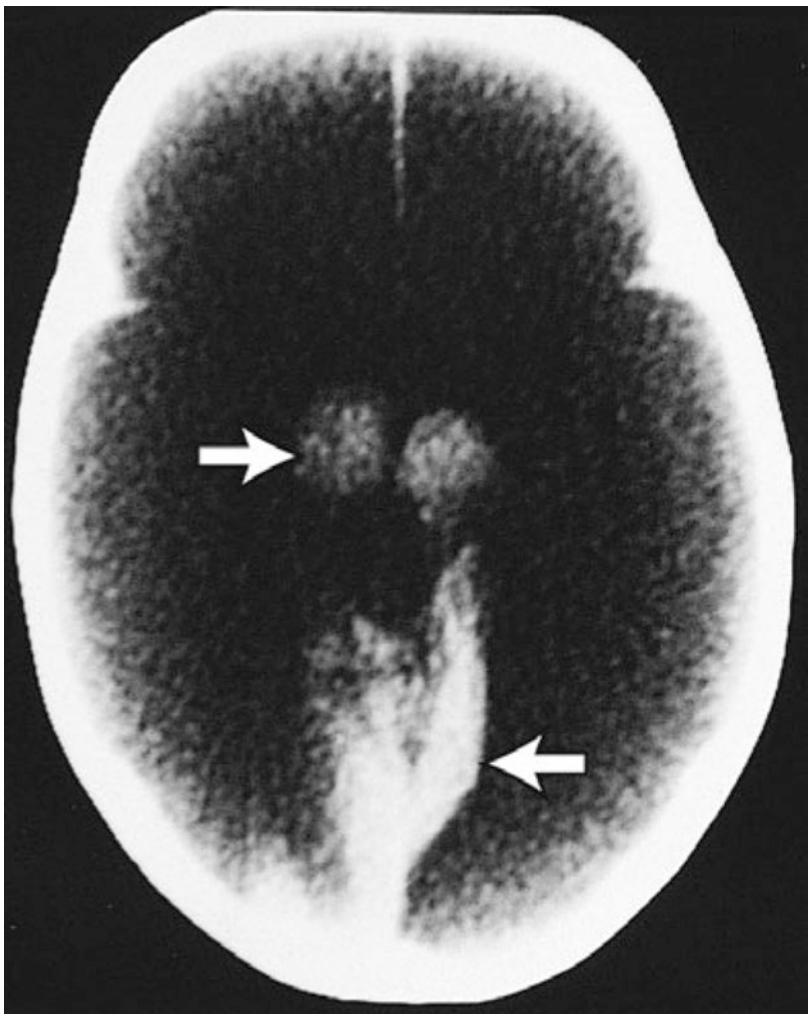

Fig. 23 CT scan of a patient with hydranencephaly. The *left arrow* indicates the intact thalamus, and the *right arrow* indicates a segment of the deep venous sinus system

Williams-Beuren Syndrome

Williams-Beuren syndrome (WBS) is a relatively common genetic disorder that causes mild to moderate developmental disability. It is easily diagnosed because of characteristic facies and a recognizable behavioral phenotype (Fig. 24). Epicanthal folds, flattened bridge of the nose, short nose with upturned nares, relatively long philtrum, and prominent lips are characteristic of the elfin facial features associated with WBS. Dental anomalies and peripheral pulmonary stenosis may also occur. Ocular features include epicanthal folds, medial eyebrow flare, strabismus, and periorbital fullness. Individuals with light-colored eyes often demonstrate a stellate pattern of the iris. The patient also exemplifies the behavioral phenotype called "cocktail party chatter," characterized by inappropriately friendly and loquacious speech. This feature often persists into adulthood, with many patients describing themselves as too trusting and easily taken advantage of. The relative preservation of verbal skills in the face of impaired reasoning and poor visual motor integration often leads to unrealistic expectations and frustration for the family until the diagnosis has been established. Medical problems in infancy include irritability, feeding difficulty, failure to thrive, constipation, and hypercalcemia. The hypercalcemia rarely persists beyond infancy, but may occasionally require control measures such as administration of calcitonin or intravenous fluids and diuretics. Cardiovascular anomalies include supravalvular aortic or pulmonic stenosis, but ventricular septal defects and patent ductus arteriosus may also be seen. Hypertension, with or without renal anomalies, may be encountered; indeed, some infants with WBS are diagnosed upon presentation with hypertensive encephalopathy. A history of hyperacusis is often elicited on direct questioning of the parents.

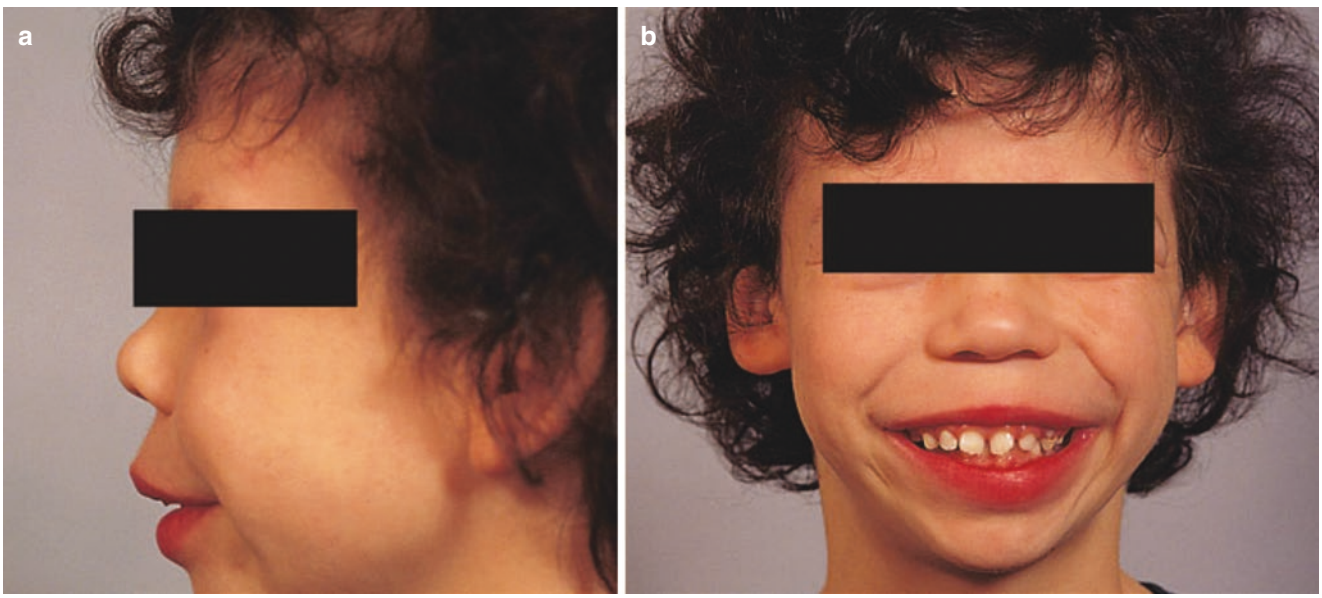

Fig. 24 Williams-Beuren syndrome (WBS) in an 8-year-old child. (**a**) WBS is easily diagnosed because of characteristic facies and a recognizable behavioral phenotype. (**b**) Epicanthal folds, flattened bridge of the nose, short nose with upturned nares, relatively long philtrum, and prominent lips are characteristic of the elfin facial features associated with WBS